DOI: 10.1002/cbic.200800836

Fine-Tuning of Catalytic Properties of Catechol 1,2-Dioxygenase by Active Site Tailoring

Raffaella Caglio,[a] Francesca Valetti,*[a] Patrizia Caposio,[b] Giorgio Gribaudo,[b] Enrica Pessione,[a] and Carlo Giunta[a]

Catechol 1,2-dioxygenases and chlorocatechol dioxygenases are Fe^{III}-dependent enzymes that do not require a reductant to perform the *ortho* cleavage of the aromatic ring. The reaction mechanism is common to the two enzymes, and active-site residues must play a key role in the fine-tuning of specificity. Protein engineering was applied for the first time to the catalytic pocket of a catechol 1,2-dioxygenase by site-specific and site-saturation mutagenesis with the purpose of redesigning the pocket shape for improved catalysis on bulky derivatives. Mutants were analysed for changes in kinetic parameters: variants for residue 69 show an inversion of specificity with a preference towards 4-chlorocatechol (decrease of K_M by a factor of 20) and activity on the rarely recognised substrate 4,5-dichlorocatechol, thus creating a novel, engineered chlorocatechol dioxygenase. A L69A substitution conveys gain-of-function activity towards 4-*tert*-butylcatechol. Mutations of position 72 enhance k_{cat} towards chlorinated substrates. The biphasic Arrhenius plot observed in A72S suggests the involvement of a dynamic switch in the fine regulation of the enzyme.

Introduction

Oxygenases are key enzymes in degrading toxic compounds (pollutants, drugs and other xenobiotics) and therefore their potential application as biocatalysts is of great interest.[1] A protein-engineering approach has been demonstrated to achieve successful results in going beyond the limits in activity, protein stability and range of recognised substrates of naturally occurring oxygenases.[2,3,4] Moreover a systematic active site tailoring approach can provide insight in the enzyme mechanism of substrate recognition and catalysis by finely tuning the kinetic properties and by highlighting the structure–function interplay that underpins the observed effects.

Catechol dioxygenase and chlorocatechol dioxygenase are key enzymes in the detoxification cascade of aromatic compounds because they catalyse the reaction that cleaves either the intradiol or the proximal extradiol bond of catechol; this results in ring opening and thus de-aromatises the substrate. Catechol and its substituted derivatives (particularly mono- and polychlorinated) are produced as a central catabolites from converging routes of aromatic degradation pathways, including highly recalcitrant compounds such as polychlorinated biphenyls (PCBs), polynuclear aromatic hydrocarbons (PAHs), aniline, dibenzofuran, and dibenzo-*p*-dioxin.[5–9] During the degradation of these recalcitrant molecules the production of monoaromatic diols can be repeated at several steps.[7] Among these, the halogenated derivatives are of great relevance, given their high toxicity and persistence in the environment.[10] It has also been reported that chlorinated catechols can competitively inhibit the bacterial oxygenases that operate the first steps of biphenyl detoxification;[11] therefore the removal of chlorinated catechols from contaminated sites might enhance the efficiency of microbial PCB removal systems.

More importantly chlorocatechols in soil and water are derived from chlorophenols and chlorobenzenes that are largely widespread pollutants due to the extensive release in the environment of solvents, herbicides and industrial wastes.[12–14] Both catechol and chlorocatechols have been reported to produce toxic effects such as irritation, convulsions and systemic disorders. Direct effects on DNA as carcinogenic and teratogenic molecules have also been observed.[15–18] Therefore both the detection and the removal of catechols and chlorinated catechols from the environment (soil and waters) is of paramount importance.

Catechol 1,2-dioxygenase and chlorocatechol 1,2-dioxygenase, the enzymes that operate the aromatic cleavage through the *ortho* intradiolic pathway, share a similar catalytic mechanism. The presence of an Fe^{III} atom enables the enzyme to insert two hydroxyl groups that are derived from molecular oxygen without the need of a reducing equivalent supply. All the enzymes of the family are dimers and contain associated lipids whose role is still uncertain.[19–21] The recent characterisation of the crystal structure of two chlorocatechol dioxygenases[20,22] and the availability of the structures of catechol 1,2-dioxygenase from *Acinetobacter calcoaceticus* ADP1 (1,2-CTD)[21] and from *Pseudomonas arvilla*[19] allowed us to highlight and structurally align some key residues that define the active-site

[a] *Dr. R. Caglio, Dr. F. Valetti, Prof. Dr. E. Pessione, Prof. Dr. C. Giunta*
Department of Human and Animal Biology, University of Torino
Via Accademia Albertina 13, 10123 Torino (Italy)
Fax: (+39) 011-6704508
E-mail: francesca.valetti@unito.it

[b] *Dr. P. Caposio, Prof. Dr. G. Gribaudo*
Department of Public Health and Microbiology, University of Torino
Via Santena 9, 10126 Torino (Italy)

pocket for recognition of catechol and its chlorinated derivatives (Figure 1). The structure–function correlation nevertheless is not so obvious, because an insertion of six amino acids is present in catechol dioxygenase compared to chlorocatechol dioxygenase around residues 73–76 in 1,2-CTD from ADP1 (corresponding to residue 52 in 4-CCD from *Rhodococcus opacus* 1CP). The most significant substitutions in the catalytic pocket are represented by Asp52/Pro76, Ala53/Gly77, Phe78/Leu109 and Cys224/Ala254 (*Rho* 1,2-CCD/*Ac* 1,2-CTD), whereas other residues are conserved, although backbone and lateral chains shifts are observed. Sequence and structural alignments stressed that some conserved positions are crucial for substrate recognition, and that amino acid substitution can tune the specificity of recognition and catalysis on catechol and chlorinated catechols. In particular, amino acids in positions 48, 52 and 73 are relevant to differentiate the substrate specificity of the two highly homologous chlorocatechol dioxygenases CbnA and TcbC, which recognise 3,5-dichlorocatechol and 3,4-dichlorocatechol respectively.[23] Other structural differences can account for the different turnover number in catechol dioxygenase (up to 40 s^{-1}) and chlorocatechol dioxygenase (those on 3- or 4-chlorocatechol are never higher than 4–6 s^{-1}, and only in 3-CDD does it reach 20 s^{-1} on 3- and 4-methylcatechols).[20,22]

The catechol dioxygenase that was considered here for protein engineering was cloned from the Gram-negative bacteria *A. radioresistens* LMG S-13.[24] This strain expresses a highly efficient phenol-degrading system with a multicomponent organisation that is focused on two key enzymes: 1) a multicomponent phenol hydroxylase[25–27] that is able to recognize and hydroxylate, beyond phenol, molecules that have higher degree of hydrophobicity and with bulkier substituents of the phenol ring, like cresols, monochlorophenols and naphthols; 2) a highly efficient catechol 1,2-dioxygenase (C1,2O) that was mentioned above, which is present in two homodimeric isoforms (IsoA and IsoB, k_{cat}: 48.7 and 31.3 s^{-1}) that are able to catalyse the *ortho* cleavage of the diolic aromatic ring leading to the first non-toxic metabolite, *cis–cis* muconate.[28,29] Both IsoA and IsoB sequences[30] display a high identity (80 and 50% respectively) with catechol 1,2-dioxygenase (1,2-CTD) of *A. calcoaceticus* ADP1, whose crystallographic structure is available.[21]

We report the effect of mutation on the crucial active-site residues (Leu69 and Ala72; Figure 1) of IsoB from *A. radioresistens* S13, which is expressed as a recombinant protein from *E. coli* BL21 (DE3). The aim was to tune the substrate specificity in favour of chlorinated substrates to obtain valuable variants both for theoretical studies on the enzyme and for applicative purposes; we present for the first time a protein-engineering strategy on a catechol 1,2-dioxygenase.

Results and Discussion

Mutants design and production

The aim of the protein-engineering strategy was to identify residues in catechol 1,2-dioxygenases that might hinder the recognition of chlorinated derivatives by steric effects and to mutate them to redesign the pocket shape and properties. The protein catechol 1,2-dioxygenase IsoB from *A. radioresis-*

```
A  C1,2O        ---------MNRQQIDALVKQMNVDTAKGPVDERIQQVVVRLLGDLFQAIEDLDIQPS   49
B  1,2-CTD      ---MEVKIFNTQDVQDFLRVASGLEQEG-GNPRVKQIIHRVLSDLYKAIEDLNITSD   53
C  1,2-CTD      ---MSIKVFGTKEVQDLLKAATNLEGKG-GNARSKQIVHRLLSDLFKAIDDLDITPD   53
D  1,2-CTD      ---MTVKISHTADIQAFFNQVAGLDHAE-GKPRFKQIILRVLQDTARLIEDLEITED   53
E  3CCD         ----------------------------------MSTDRTGNIVGKMIAAINAVIKDEKVSYS   29
F  4CCD         ---------------------------MANTRVIELFDEFTDLIRDFIVRHEITTP   29
G  CCD CbnA     ----------------------------MNERVKQVASALVDAIQKTLTEQRVTEE   28
H  CCD TcbC     ----------------------------MNERVKQVASALVDAIQKTLTEQRVTEE   28
I  CCD          ----------------------------MNERVKQVASALVDAIQKTLTEQRVTEE   28
J  CCD          ----------------------------MDKRVAEVAGAIVEAVRKILLDKRVTEA   28
K  HQD2         MVIKKE-------SDLTAAVLAVMNRTEEPRLREILVAMVKHLHAFVREVRLTEV   48
L  HQD2         MTSEEESAAAPAAGSFDEHNLTQTVLQSVAGAKDPRVKQISEALIRHLHAFIREIEPTEA   60

A  C1,2O        EVWKGLEYLTDAG--QANELGLLAAGLGLEHYLDLRADEADAKAGITGGTPRTIEGP  104
B  1,2-CTD      EYWAGVAYLNQLG--ANQEAGLLSPGLGFDHYLDMRMDAEDAALGIENATPRTIEGP  108
C  1,2-CTD      EVWAGVNYLNKLG--QDGEATLLAAGSGLEKYLDIRLDAADKAEGIEGGTPRTIEGP  108
D  1,2-CTD      EFWHAVDYLNRLG--GRNEAGLLAAGLGIEHFLDLLQDAKDAEAGLGGGTPRTIEGP  108
E  3CCD         EYKASTGWLISVG--EQNEWPLFLD-----VFFEHAIESVAAESNRGSQSSIQGP   77
F  4CCD         EYETIMQYMISVG--EAGEWPLWLD-----AFFETTVDSVSYGKGNWTSSAIQGP   77
G  CCD CbnA     EWRAGVGYMMKLA--EAKEMALLLD-----VFFNHTIVDLKAQATRGSTPAIQGP   76
H  CCD TcbC     EWRAGVGYMMKLA--EAKEVAVLLD-----AFFNHTIVDLKAQATRGSRPAMQGP   76
I  CCD          EWRAGVGYMMKLA--EAKEMALLLD-----AFFNHTIVDLKAQATRGSTPAIQGP   76
J  CCD          EYRAGVDYLTEVA--QTRETALLLD-----VFLNSTIIEGKAQRSRTSAPAIQGP   76
K  HQD2         EFREATAMLNEIGKLHTDQHNEFVLMAGSLG--VSSLVCLLNNGDRGQTETSQSLLGP  104
L  HQD2         EWGAAIEFLTKTGHMCTDTRQEFILLSDVLG--VSMLVDAINHRLPG-RATETTVFGP  115
```

Figure 1. Amino acid sequence alignments; the residues that are relevant for the present work are highlighted in grey. A) Catechol 1,2-dioxygenase *Acinetobacter radioresistens* S13 (NCBI protein accession Q9F103), B) catechol 1,2-dioxygenase *Acinetobacter sp.* ADP1 (NCBI protein accession P07773), C) catechol 1,2-dioxygenase *Acinetobacter lwoffii* (NCBI protein accession O33948), D) catechol 1,2-dioxygenase *Pseudomonas arvilla* C-1 (NCBI protein accession Q51433), E) chlorocatechol 1,2-dioxygenase *Rhodococcus opacus* 1CP (NCBI protein accession Q8G9L3), F) chlorocatechol 1,2-dioxygenase *Rhodococcus opacus* 1CP (NCBI protein accession O67987), G) chlorocatechol 1,2-dioxygenase mutant CbnA *Ralstonia eutropha* (NCBI protein accession Q9WXC8), H) chlorocatechol 1,2-dioxygenase mutant TcbC *Pseudomonas sp.* (strain P51) (NCBI protein accession P27098), I) chlorocatechol 1,2-dioxygenase *Pseudomonas nitroreducens* (NCBI protein accession A1E5L2), J) chlorocatechol 1,2-dioxygenase *Pseudomonas putida* (NCBI protein accession P11451), K) hydroxyquinol 1,2-dioxygenase *Rhizobium sp.* NGR234 (NCBI protein accession 36959091), L) hydroxyquinol 1,2-dioxygenase *Sphingomonas sp.* (NCBI protein accession 4007783). The alignment was generated by using ClustalW.

tens S13[30,31] was chosen for its good stability and high catalytic activity on catechol and for its cleavage of chlorinated catechol ring derivatives with relatively high rate constants for a catechol dioxygenase. The recombinant expression in *E. coli* BL21 (DE3) allowed us to pursue a protein-engineering approach to redesign the active site for enhanced catalysis on catechol derivatives. A model of the enzyme (Figure 2) was obtained by homology by using the crystal structure of 1,2-CTD from *Acinetobacter* ADP1 as a template, given the high level of identity (50% on the overall sequence, close to 90% in the active-site region). The quality of the obtained model (Figure 2) was judged to be adequate for our purposes, and key residues were identified that define the active-site pocket shape. The attention was focused on residues that would interact unfavourably with catechol derivatives with bulky substituents in position 4. The residues that were selected for mutagenesis were: Leu69 (corresponding to the conserved residue numbered 73 in 1,2-CTD) and residue 72 (structurally homologous to residue 76 in 1,2-CTD and to residue 52 in chlorocatechol dioxygenases; Figure 1). Although the Leu is conserved in most reported enzyme sequences, it is present in a region that might have a fundamental role in substrate specificity and preference, and it could, if mutated to a less-bulky although still hydrophobic residue, redesign the shape of the active site to guarantee a novel route, alternative to those defined by evolution, for recognition of chlorinated aromatic substrates and catechols with bulky substituents. The Ala72 is atypical when compared to the Pro76 that is present in 1,2-CTD[21] and to the corresponding residue in the IsoA of *A. radioresistens* (also a Pro residue).[30] Mutant design was approached both by site-specific mutagenesis to generate the mutants L69A and the double mutant L69G A72G, and by site-saturation mutagenesis (SSM) coupled to the QuikChange technique by introducing a NN(G/T) codon in the mutated primer at position 72. The SSM approach allowed exploration of the alternative amino acids for position 72 that might affect the kinetic parameters and convey on the enzyme enhanced activity towards recalcitrant and chlorinated compounds.

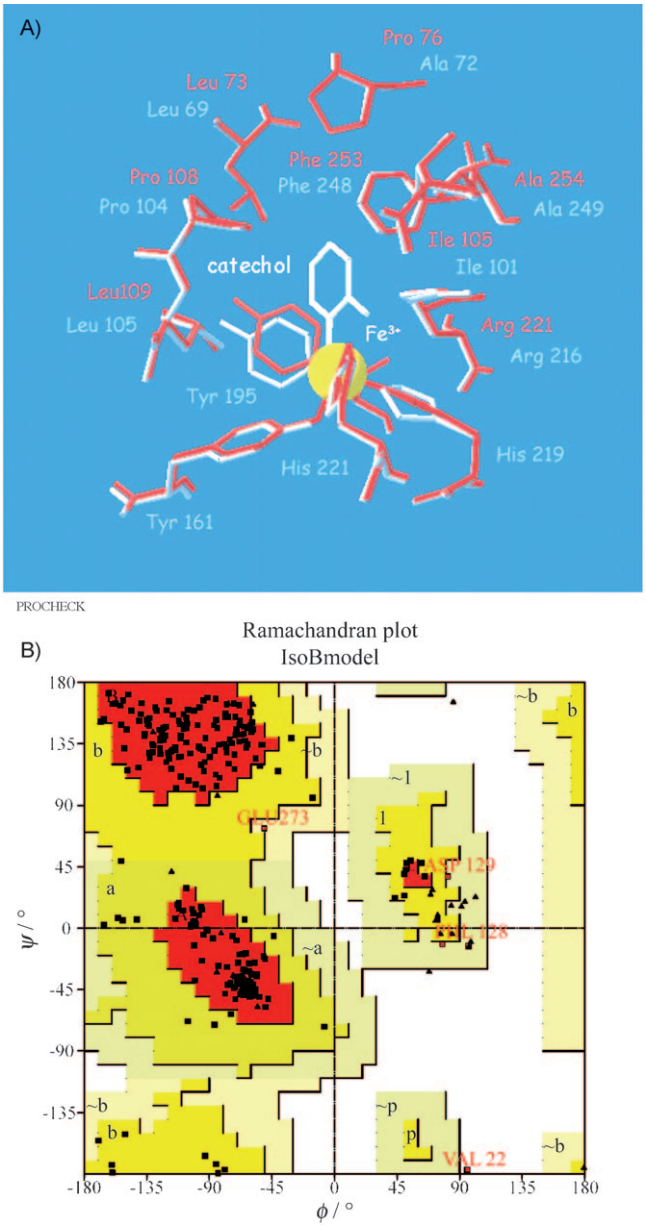

Figure 2. Model of catechol 1,2-dioxygenase from *A. radioresistens* S13. A) Structural alignment of active-site pocket residues of modelled C1,2O IsoB from *A. radioresistens* S13 and of the crystal structure of C1,2-CTD from *Acinetobacter* ADP1, which was used as a template. Relevant residues of 1,2-CTD are indicated in red (Leu73, Pro76, Ile105, Pro108, Leu109, Arg221, Phe253 and Ala254), the corresponding residues in C1,2O IsoB model (Leu69, Ala72, Ile101, Pro104, Leu105, Tyr161, Tyr195, Arg216, His219, His221, Phe248 and Ala249) are indicated in pale blue. The Fe^{III} atom is in yellow, catechol in white. B) Ramachandran plot of the entire C1,2O IsoB model that was obtained from Procheck.

The 71 colonies obtained from the QuikChange procedure were screened for the mutation insertion, by digestion of plasmid DNA with NheI as described in the Experimental Section, and 20 clones were found to be positives. The selected clones were assayed for protein expression and activity in small-scale cultures. Table 1 reports the results with highlighted selected clones and protein variants that were further analysed in this work (in bold).

The selected mutants were purified to homogeneity, and the purity was evaluated from the concentration ratio (calculated at 280 nm for the protein moiety and 430–440 nm for the specific, coordinated iron bond)[31] to ensure that the protein was in its holoform.

All mutants, with the exception of A72D, gave a value of the above-mentioned ratio close to one, as expected for the holoprotein.

Kinetics, substrate specificity and gain-of-function

The kinetic parameters K_M and k_{cat} and the specificity constants k_{cat}/K_M were determined for the selected SSM mutants, for L69A and L69G A72G, on the range of compounds shown, and compared to the value for the WT recombinant protein (Table 2). The WT was confirmed to have a high turnover number towards catechol ($24 \pm 0.36\ s^{-1}$); this is in line with the literature data on the nonrecombinant enzyme.[31] A basal activity on 4,5-dichlorocatechol was measured for WT. The recog-

Table 1. SSM A72 clones.

Clone	Variant	Codon	Expressed	Catechol	3-Methylcatechol	4-Methylcatechol	4-Chlorocatechol
SSM5	A72K	AAG	+	–	–	–	–
SSM9	A72N	AAT	+	+	+	+	+
SSM14	A72T	ACG	+	+	+	+	+
SSM15	**A72S**	**ACT**	+	+	+	+	+
SSM17	A72T	ACG	+	+	+	+	+
SSM23	–	–	+	n.d.	n.d.	n.d.	n.d.
SSM24	–	–	+	n.d.	n.d.	n.d.	n.d.
SSM26	–	–	+	n.d.	n.d.	n.d.	n.d.
SSM27	A72S	AGT	+	+	+	+	+
SSM34	–	–	+	+	+	+	+
SSM36	**A72G**	**GGT**	+	+	+	+	+
SSM37	A72T	ACT	+	+	+	+	+
SSM45	**A72D**	**GAT**	+	+	+	+	+
SSM47	–	–	+	+	+	+	+
SSM50	A72N	AAT	+	+	+	+	+
SSM57	–	–	+	+	–	+	+
SSM62	A72P	CCG	+	+	+	+	+
SSM63	–	–	+	+	+	+	+
SSM64	A72S	AGT	+	+	–	+	+
SSM68	**A72N**	**AAT**	+	+	+	+	+

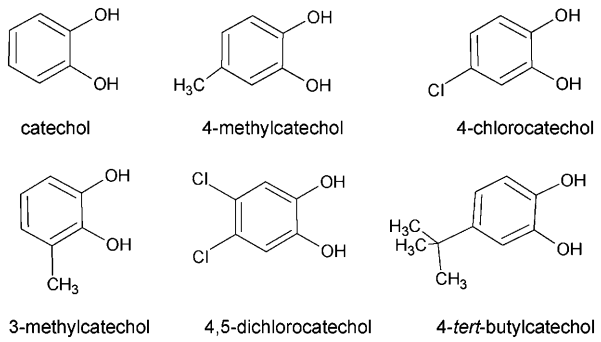

nition and catalysis of this substrate is rather rarely observed among chlorocatechol dioxygenases,[32] and to our knowledge it has not been previously reported for a catechol dioxygenase. The activity on 4,5-dichlorocatechol was observed on all active variants, albeit with different k_{cat} values; substrate consumption and chlorinated muconate production was confirmed by HPLC analysis, as shown in a representative chromatogram with variant L69A (Figure 3).

The data reported in Table 2 confirmed that the selected residues 69 and 72 are highly relevant for substrate recognition and catalysis, as expected from in silico structural alignments with known crystal structures of catechol dioxygenases, and are in line with the literature data.[21,19]

In particular, substitution in position 69 of leucine with alanine dramatically affects the K_M for catechols with bulky substituents in position 4, by decreasing the K_M for 4-methylcatechol by a factor of four, and for 4-chlorocatechol by a factor close to 20. The trend is confirmed in the double mutant, L69G-A72G in which the obtained values of K_M for 4-methylcatechol and 4-chlorocatechol are consistent with an additive effect of the two mutations. In fact the A72G substitution by itself decreases the K_M towards 4-methylcatechol, but a slight increase is observed for 4-chlorocatechol. Therefore the mutation of position 69 seems crucial for a higher affinity towards 4-substituted catechols. It is to be noted that Leu69 can be structurally aligned with highly conserved identical residues in several crystal structures of both chlorocatechol and catechol dioxygenases. The mutation to alanine is not severely destabilising for the enzyme, as confirmed by the stability data presented in Table 3, but it represents a mutational space not explored by nature in the selection and optimisation of these enzymes. The gain of function of the L69A variant for recognition and catalysis of 4-*tert*-butylcatechol (Figure 4) suggests that the increase in size of the active-site pocket caused by the Leu-to-Ala substitution might allow the binding of rather bulky substituents in the 4-position, which would be oriented towards position 69. This is also in line with a decreased K_M for the 4-substituted catechols in L69A, as was already discussed and reported in Table 2. The net result of mutation in both mutants affecting position 69 is an inversion of specificity (calculated as k_{cat}/K_M) compared to WT from catechol to 4-chlorocatechol, thus defining a new structural route to select for a chlorocatechol dioxygenase-like enzyme instead of a catechol dioxygenase.

Mutations in position 72, although they do not cause such an inversion of substrate specificity, are more interesting for the enhancement of k_{cat} towards chlorinated substrates. A two-fold k_{cat} enhancement on 4-chlorocatechol is observed both in A72G and A72S. Also in A72S an increase in activity by 33% was recorded towards 4,5-dichlorocatechol. The activity towards catechol is maintained at good levels (16 s^{-1}) with a five-fold increase of K_M. The K_M increase was also observed in both A72S and A72G towards 4-chlorocatechol, but here the value was only three-fold higher.

The activity detected in both mutants A72N and A72D (mutant A72K was found completely inactive) is interesting considering that by structural alignment with chlorocatechol

Table 2. Kinetic data for wild-type and six purified mutant enzymes.

	WT	L69A	L69G A72G	A72G	A72S	A72D	A72N
k_{cat} [s^{-1}]							
catechol	24.2 ± 0.4	4.42 ± 0.19	3.93 ± 0.17	13.6 ± 2.6	16.0 ± 0.1	0.304 ± 0.029	0.0625 ± 0.0040
3-methylcatechol	1.590 ± 0.002	0.526 ± 0.027	n.d.	n.d.	n.d.	n.d.	n.d.
4-methylcatechol	5.45 ± 0.05	0.729 ± 0.046	1.22 ± 0.09	5.51 ± 0.66	7.39 ± 1.55	0.520 ± 0.035	0.713 ± 0.063
4-chlorocatechol	0.83 ± 0.14	0.347 ± 0.015	0.93 ± 0.09	1.74 ± 0.16	1.74 ± 0.09	0.307 ± 0.018	0.207 ± 0.010
4,5-dichlorocatechol	0.177 ± 0.013	0.174 ± 0.020	0.193 ± 0.033	0.174 ± 0.018	0.235 ± 0.021	0.062 ± 0.001	0.079 ± 0.022
4-*tert*-butylcatechol	0	0.061 ± 0.014	n.d.	0	0	0	0
K_M [μM]							
catechol	2.04 ± 0.30	5.76 ± 0.95	42.8 ± 5.8	9.3 ± 1.0	10.0 ± 1.9	69.1 ± 15.5[b]	2.35 ± 0.58
3-methylcatechol	2.25 ± 0.30	5.95 ± 0.95	n.d.[a]	n.d.[a]	n.d.[a]	n.d.[a]	n.d.[a]
4-methylcatechol	53 ± 7	12.8 ± 2.2	2.84 ± 0.70	10 ± 1.2	213 ± 32	93.6 ± 15.8[b]	435 ± 87
4-chlorocatechol	1.98 ± 0.30	0.101 ± 0.033	2.42 ± 5.20	6.13 ± 0.7	6.54 ± 3.43	208.1 ± 26.4[b]	50.1 ± 6.5
k_{cat}/K_M [$M^{-1} s^{-1}$]							
catechol	11 800 000	780 000	90 000	1 460 000	1 600 000	4000	26 600
3-methylcatechol	710 000	88 000	n.d.[a]	n.d.[a]	n.d.[a]	n.d.[a]	n.d.[a]
4-methylcatechol	100 000	56 700	430 000	551 000	34 700	5600	1640
4-chlorocatechol	420 000	3 440 000	380 000	280 000	417 000	1500	4140

[a] n.d. = not determined. [b] These data are purely indicative, given the presence of a % of apo-protein.

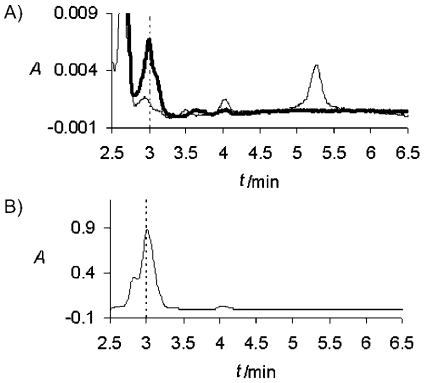

Figure 3. RP-HPLC analysis of reaction products and reactants on a representative C1,2O L69A reaction on 4,5-dichlorocatechol. A) The thin line represents the HPLC chromatogram obtained from the mock reaction mixture at 17 h; the 4,5-dichlorocatechol specific peak is at a retention time of 5.2 min; the thick line represents the HPLC chromatogram of the reaction products obtained after 17 h. The specific peak (with a typical shoulder) at a retention time of 3.0 min is the 3,4-dichloromuconic acid. B) The HPLC trace shows the standard reaction product 3-chloromuconate obtained by the enzyme degradation of 4-chlorocatechol.

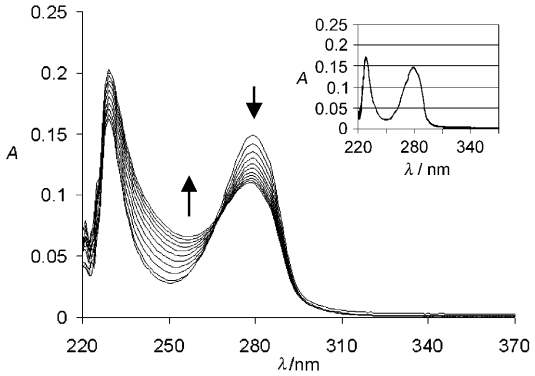

Figure 4. Spectral changes recorded upon catalytic activity of the L69A mutant on 4-*tert*-butylcatechol measured for 10 min. The arrows indicate the changes due to consumption of substrate (↓) and the correspective production (↑) of product. Inset: spectral profile of the same reaction conduced on wild-type. In both L69A and WT reaction mixture the substrate final concentration was 200 μM and the enzyme final concentration was 0.26 μM.

dioxygenase an Asp residue (Asp52) was suggested to correspond to position 76 of ADP1 and 72 of our model.[20] This single substitution, given the presence of a six amino acid insertion in that region, is not determinant for inversion of substrate specificity due to the K_M increase (Table 2), although the dramatic decrease in k_{cat} towards catechol (by 2–3 orders of magnitude) was not measured on 4-chloro and 4,5-dichloro-substituted substrates (k_{cat} 20 to 50% of the WT values) and on 4-methyl derivatives (10–15% of the WT value).

Table 3. Stability data (pH, temperature and iron removal versus activity) for WT and selected mutants.

	Temperature dependence of activity $T_{50\%}$ [°C]		pH dependence of activity $pH_{50\%}$	Iron removal k_{rem} [h^{-1}]
Substrate	Catechol	4-Chlorocatechol	Catechol	Catechol
WT	49.4 ± 1.01	51.8 ± 2.17	6.89 ± 0.05	0.38 ± 0.06
L69A	43.0 ± 0.80	49.9 ± 0.42	7.07 ± 0.07	0.33 ± 0.90
A72G	38.6 ± 1.63	49.0 ± 0.41	7.44 ± 0.05	0.37 ± 0.07
A72S	46.1 ± 0.40	49.2 ± 3.62	7.53 ± 0.06	0.36 ± 0.08[a] 3.12 ± 0.18[b]
L69G A72G	32.7 ± 0.54	40.1 ± 0.69	7.49 ± 0.25	4.58 ± 0.57

[a] Trend 1: value obtained by fitting the datapoints from 100 to 50% residual activity. [b] Trend 2: value obtained by fitting the datapoints from 50 to 0% residual activity.

Mutant stability: specific effect of variants

The mutant stability was determined on the most promising variants by analysing the temperature and pH dependence of the activity. By fitting the decrease observed in catalytic activity upon temperature increase to a sigmoid curve, the flexus points were calculated and are referred to as $T_{50\%}$. As reported in Table 3, the mutations did not severely affect the stability of the enzymes with the exception of the double mutation L69G-A72G, which is not surprising given the severe reduction in the hydrophobicity and size of the Leu residue and the related destabilisation expected. A decrease in $T_{50\%}$ was also observed in A72G, therefore a synergistic combination might cause, in the double mutant, the reported effect. All variants display a higher $T_{50\%}$ when using 4-chlorocatechol as a substrate. The pH dependence shows a maximum of activity at basic pH (8 and higher) and a decrease at more acidic pH for all variants, with a sigmoid curve of dependence and with flexus points ($pH_{50\%}$) at 7–7.5, which are not varied by mutations. The iron removal rate constants k_{rem} of the WT and mutants were also calculated by fitting the activity decay in time to an exponential curve upon incubation with a chelating resin, as explained in the Experimental Section and as previously reported.[33] Controls were performed with mock reactions without the chelating resin, and no activity decrease was observed within the time span of the experiment. The k_{rem} are reported in Table 3, the data and fitting are plotted in Figure 5.

As expected, the double mutant is heavily destabilised; this is consistent with a suggested effect of the hydrophobic residues on iron retention in the catalytic pocket.[33] A peculiar behaviour was observed for A72S: a change in the exponential curve is observed when the residual activity is around 50%, with an increase in metal-removal rate constant; this suggests that at 50% inactivation a massive destabilisation occurs that enhances the iron release. It can be hypothesised that at 50% enzyme inactivation either 50% of the dimers are in the apoform and inactive and 50% are fully active in the holoform (highly unlikely), or that statistically dimers have in the majority one protomer in the apo and one protomer in the holoform. In this second case, it can be suggested that such dimers are destabilised and that the apo-protomer can cause, through the interface of dimerisation, a rearrangement of the holoprotomer with an abrupt decrease in iron retention in the active-site pocket. The fact that this is observed only in the A72S variant (the only mutation that introduces a novel H-bond donor/acceptor group compared to WT) suggests that this rearrangement can be stabilised and/or enhanced by the possible reorientation of the Ser residue and a switch in the H-bonding. This biphasic behaviour of A72S will be discussed further.

Effect of variants on E_a

The profile of the temperature-dependent activity increase was analysed in all variants to determine the activation free energy, which is calculated on the basis of the k_{cat}. The Arrhenius plot thus obtained describes the free energy of transition from the ES to the ES* state.[34] For each mutant only the increasing k_{cat} values were used for the E_a calculation in the typical temperature range that was analysed by starting from 10 °C. By comparing the energy that is required for the transition, with catechol as a substrate, it was observed that the value is higher for the WT than for the mutant in all cases except for mutant A72S (Figure 6 and Table 3). A peculiar aspect is that the lowering of the activation energy precisely follows the enlargements of the active-site pocket, with the lowest value (1343 cal mol^{-1}) obtained in the L69G A72G mutant. The value for A72S is consistently identical to the WT value given that no enlargement of the active site is expected by mutating an alanine to a serine.

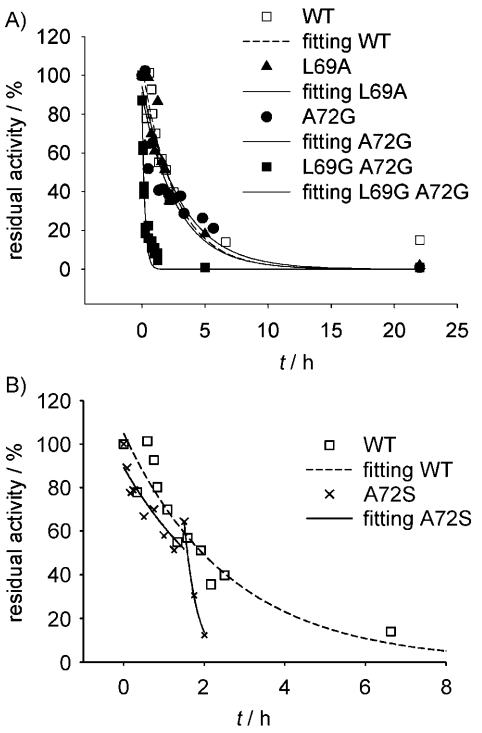

Figure 5. Demetallation curves. Profile of residual activity (evaluated on catechol as a substrate) versus time during iron removal promoted by enzyme incubation with Amberlite IRC 50 resin. The data points were fitted to an exponential decay. A) WT versus mutant L69A, L69G A72G, A72G. B) WT versus mutant A72S.

The lowering of E_a is not reflected in a k_{cat} increase; this implies that the measured E_a refers to the reorganizational energy of each variant upon catalysis. The catalytic process of C1,2O is in fact a multistep process, but here only a specific step was taken into account. This suggests that a lower energy is necessary to rearrange the enzyme upon transition, if the substrate is located in a pocket that is larger than the optimal one for the substrate itself. This is possibly linked to decreased complexity of the interaction between catechol and the mutants' active sites as compared to the precise interaction geometry that is required for the WT catalysis; the interactions required for WT catalysis are more demanding in terms of rearrangement energy. The interaction of the WT and mutants with bulkier substrates, which are not optimally recognised by the WT, implies that the enzyme has alternative strategies for achieving an optimal substrate orientation and catalysis in which

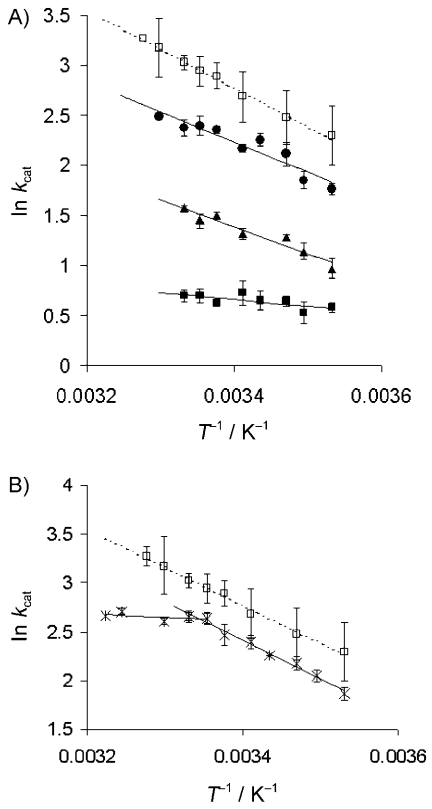

Figure 6. Arrhenius plots were obtained by fitting to the linear form of the Arrhenius equation $\ln k_{vel} = -E_a/RT + \ln A$. The value of k_{vel} is expressed as the turnover number on catechol as a substrate for A) WT (○) versus L69A (▲), L69G A72G (■), A72G (●) and B) WT (□) versus A72S (×). The data are the average of at least three independent experiments.

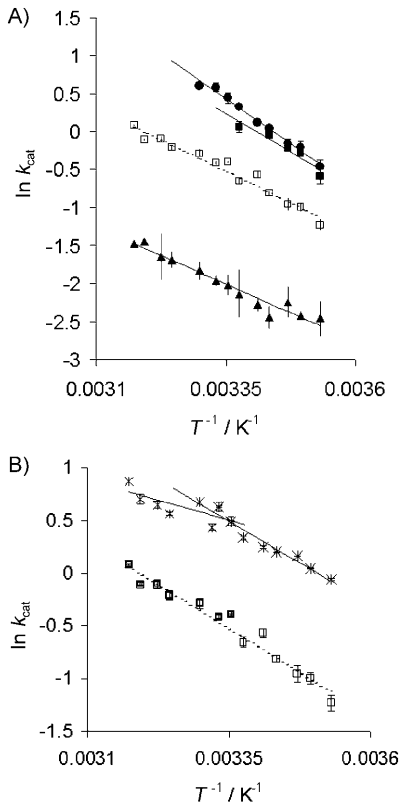

Figure 7. Arrhenius plots obtained for k_{vel} expressed as turnover number on 4-chlorocatechol as a substrate for A) WT (□) versus L69A (▲), L69G A72G (■), A72G (●) and B) WT (□) versus A72S (×). The data are the average of at least three independent experiment.

no dependency of E_a versus pocket size was observed (Figure 7 and Table 4).

The Arrhenius plot for mutant A72S could not be fitted to a linear trend and only biphasic behaviour could account for the observed data. The break-point is markedly defined when catechol is used as a substrate. Break-points in the Arrhenius plot, although often controversial, can be observed in several membrane-bound and soluble enzymes.[35–37] A possible explanation for such a break in the linear Arrhenius plot is the presence of two conformational states that are both catalytically competent.[38,39] Other possible explanations for the non-linearity of these plots are thermal inactivation or a pH change in the reaction buffer upon temperature. These latter causes were evaluated by verifying the stability of A72S to temperature and pH. No destabilising effect was observed in the range and reaction conditions that were used for the assay. It should also be noted that the protein stability of A72S and WT is very similar under the same reaction conditions, but the behaviour of the two protein variants in the Arrhenius plot is markedly different.

The temperature at which the discontinuity is observed (25–27 °C) could be consistent with a structural transition triggered by the phospholipid;[37,40] which is associated with the N-terminal helices of each protomer (helices 2–4 and 6). These helices define both the protomer–protomer interaction region and, through helix 4 (in which Leu69 is inserted), the edge of the active-site region.[20,21] A phospholipid rearrangement could determine a reshaping of the active-site pocket with an increase in size, which would be reflected in a lower E_a for the ES to ES* transition, in the range of 27–32 °C. Furthermore, because this sharp transition is only observed in A72S mutant, the transition might occur and be observed due to a stabilising effect of H-bonds involved in the re-oriented OH group of Ser72. The conformational change with an increase in the active-site pocket size that is hypothesised in this view could also be consistent with the two-fold enhancement of catalysis on 4,5-dichlorocatechol for the A72S mutant as compared to WT. All experimen-

Table 4. E_a [cal mol^{-1}].

Substrate	Catechol	4-Chlorocatechol
WT	7716 ± 920	7895 ± 426
L69A	5286 ± 474	4854 ± 1094
A72G	6353 ± 633	9932 ± 347
A72S[a]	740 ± 503	1987 ± 782
A72S[b]	7784 ± 419	6227 ± 306
L69G A72G	1343 ± 492	8032 ± 884

[a] Obtained by fitting of datapoints at temperature below the break point (10–25°C) [b] Obtained by fitting of datapoints at temperature above the break point (27–35°C).

tal determinations were performed at 30 °C, which is the temperature at which the active site should be re-shaped to allow allocation of the more bulky substrates. When using 4-chlorocatechol as a substrate, the transition, although present, is less pronounced, and there is a relatively lower decrease in E_a at temperatures in the 27–32 °C region. This would suggest, as expected, a minor effect of the active-site size increase on the reorganizational energy of the enzyme when a bulky substrate is bound. A modelling study (presently underway) suggests that A72S variant could have conformations that involve the re-orientation of the Ser in the active site. In this way, we also identified a possible rearrangement of H-bonding network involving Ser72 (Figure 8).

Conclusions

Catechol dioxygenases have recently received attention for a number of studies focusing on the elucidation of catalytic mechanism and selectivity of extradiol versus intradiol cleavage.[41–43] A random mutagenesis approach that was applied to a catechol 2,3-dioxygenase allowed the selection of variants with acquired intradiol cleavage activity.[44] Also several works were published on functional mimics of both intradiol and extradiol-cleaving enzymes.[45–47] These structure–function studies highlight the great plasticity of the enzyme active site and make these enzymes particularly promising for protein-engineering studies that aim both at a more precise characterisation of the catalytic properties and at reshaping for technological applicative purposes. To date, to our knowledge, no protein-engineering approach has been performed on catechol 1,2-dioxygenases.

The experimental data reported here demonstrate the feasibility of using active-site engineering to generate a catechol 1,2-dioxygenase with high catalytic activity and good stability.

Variants were produced that show the inversion of specificity with a preference towards 4-chlorinated catechols and a peculiar activity on the rarely recognised substrate 4,5-dichlorocatechol,[32] thus creating a novel engineered chlorocatechol dioxygenase. The mutation of a conserved residue conveys gain-of-function activity towards 4-*tert*-butylcatechol, a toxic compound found as a contaminant in cosmetic preparations, where its presence in trace amounts is allowed by European legislation.[48] No activity of natural known catechol dioxygenases on this compound has been reported previously. Changes in kinetic parameters in all variants and biphasicity in the Arrhenius plot in a single mutant A72S can shed light on the enzyme mechanism fine regulation. The hypothesised switch mechanism observed in mutant A72S is presently the starting point for further investigations on the reaction intermediates and pathways affected by the mutation, tackled by experimental and computational approach.

Experimental Section

Chemicals: All reagents used in this study were analytical grade and purchased from Sigma–Aldrich (Milan, Italy).

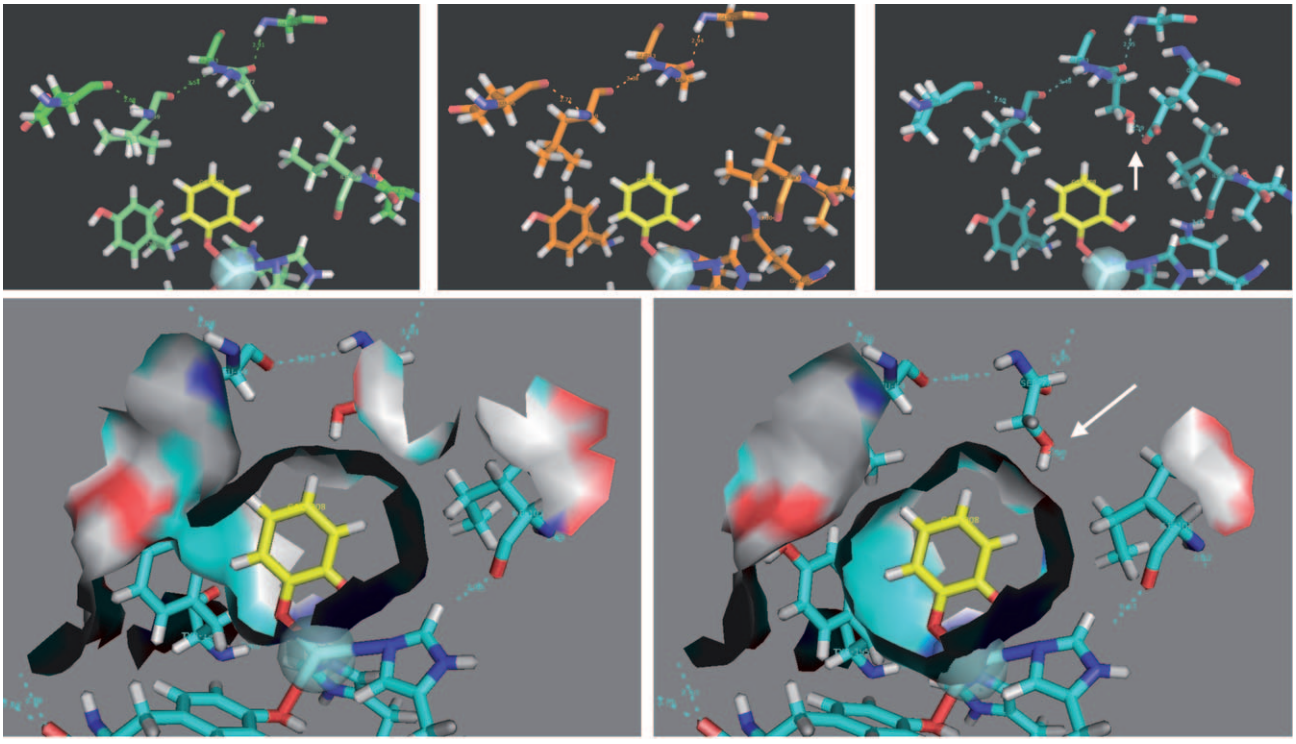

Figure 8. Active-site models obtained with Modeller and visualised with PyMol of the active-site pocket of C1,2O IsoB WT (top left), A72G (top center) and A72S (top right). The discontinuous lines are possible hydrogen bonds. The white arrow in the top right picture indicates an extra H-bond modelled for A72S. Bottom) The modelling of A72S suggests that two equally probable orientations of the Ser residue (both with high score for the model stability) can be obtained that differ in their hydrogen-bonding network and active-site cavity shape.

Modelling: The model of C1,2O IsoB sequence from *Acinetobacter radioresistens* S13 was elaborated by automated homology modelling with the 3D-JIGSAW service (http://www.bmm.icnet.uk/servers/3djigsaw) by using the crystal structure of C1,2O from *Acinetobacter calcoaceticus* ADP1 as a template.[21] The 3D structure of the obtained model was submitted to Whatcheck service (http://biotech.ebi.ac.uk:8400/) to check for angle geometry and length of bonds.[49]

The Fe^{III} atom was inserted in the active site of the model by superposition of 1,2-CTD from *Acinetobacter* ADP1 structure.

Cloning and expression of WT and mutants: A coding sequence for a His-tag domain (His_6) and IsoB DNA from *Acinetobacter radioresistens* S13 was cloned between NdeI site and EcoRI site in pET 30+ (Novagen) overexpression plasmid that contained an isopropyl β-D-thiogalactopyranoside-inducible promoter and a Kan^R gene for transformant selection.[24] Site-directed mutagenesis was performed by using the QuikChange site-directed mutagenesis system (Stratagene). To prevent primers from overlapping, the PCR reaction was performed in two steps by adding only one oligonucleotide at each step; for the mutant in position 69 (L69A) sense and antisense oligonucleotides were: forward 5′-CCA ATG AAC TCG GCG CGC TCG CTG CCG GG-3′ and reverse 5′-CCC GGC AGC GAG CGC GCC GAG TTC ATT GG-3′. The same method was used to create a double mutant L69G A72G and the sense and antisense oligonucleotide were: forward 5′-CCA ATG AAC TCG GCG GGC TCG CCG GCG GGC TCG GTC TTG-3′ and reverse 5′-CAA GAC CGA GCC CGC CGG CGA GCC CGC CGA GTT CAT TGG-3′.

Mutants in position 72 were created by the QuikChange mutagenesis system, which was adapted to site-saturation mutagenesis (SSM), and the primers used were: forward 5′-CCA ATG AAC TCG GCC TGC TAG CTN NKG GGC TCG GTC TTG-3′ and reverse 5′-CAA GAC CGA GCC CMN NAG CTA GCA GGC CGA GTT CAT TGG-3′. The underlined bases indicate a silent mutation (boldface) generating a restriction site for NheI enzyme that was used for mutant screening. **NNK** and **MNN** were degenerate codons positioned near the centre of the primer and consisted of 25% each G, C, A and T (nucleotides code: **N**) and 50% G and T (nucleotide code: **K**) or C and A (nucleotide code: **M**).[50,51]

Reaction mixtures were prepared by following the recommended QuikChange protocol.

The following PCR program was used: 94 °C (30 s) 1 cycle, 94 °C (30 s) 55 °C (1 min) 72 °C (12 min) 18 cycle, 72 °C (7 min) 1 cycle, 12 °C hold.

The amino acid sequence of the mutants was confirmed by DNA sequencing (MWG-Biotech, Germany).

Protein expression: Both wild-type and mutant plasmids were transformed into *E. coli* BL21 (DE3) competent cells by using conventional methods. The transformed *E. coli* cells were grown in Luria-Bertani (LB) broth with kanamicin (30 μg mL^{-1}) at 37 °C until the absorbance reached 0.7 at a wavelength of 600 nm; then isopropyl β-D-thiogalactopyranoside (IPTG; 1 mM) was added, and the protein expression was induced for 2 h and 30 min. The cells were harvested by centrifugation (20 min; 4 °C; 3000 *g*) and stored at −20 °C.

To confirm the presence and activity of mutants, small-scale cultures (5 mL) were grown and either induced with IPTG (I) or not induced (NI) as a control; the activity was assayed on clarified cytosolic extract of the same amount of cell lysate of I or NI.

Protein purification: For further processing, cells were thawed on ice, resuspended in resuspension buffer (40 mL of resuspension buffer for a cell pellet of 4 g wet-weight, 5 mM imidazole, 0.2 M NaCl and 20 mM Tris–HCl, pH 7.9), broken by sonication and centrifuged at 13000 *g*. All purification steps were carried out at 4 °C. The supernatant was applied to a Q-Sepharose column (GE Healthcare) and equilibrated with 50 mM HEPES pH 8.0. Proteins were eluted with a linear gradient of 0 to 500 mM Na_2SO_4 in this buffer. The pinkish fractions that contained the desired activity were combined, concentrated, and desalted on an Amicon filtration unit with a 10000 Da exclusion membrane (Millipore). The purified protein was stored at −20 °C.

The amount of holoprotein was calculated by analysing the absorbance spectrum at 430–440 nm by using the reported extinction coefficient.[31,52]

Enzyme activity assay: *Catalytic activity.* The catalytic activity was assayed by spectrophotometric measurement (Agilent 8453 UV/visible) of absorbance increase at 260 nm due to the conversion of catechol into *cis–cis* muconic acid. All experiments were carried out at 30 °C and the activities were measured in triplicate. The assay was typically performed in 50 mM HEPES buffer (1 mL, pH 8.0) by using 0.2 mM as final concentration of catechol (or catechol derivatives).

Kinetic parameters: The kinetic parameters (K_M) were determined by using a substrate concentration from 1 μM to 1 mM at 30 °C in triplicate (enzyme concentration 100 nM) and the data were fitted to the Michaelis–Menten model by a non-linear least-squares fitting program.

pH and temperature influence on activity: The enzyme activity was determined after an acclimation time (3 min) at various temperatures (10°–60 °C) in 50 mM HEPES buffer solution (pH 8.0).

The optimum pH was determined by measuring the activity at 30 °C over the pH range of 5.5–10.0 by using the following buffers: MES–NaOH (pH 5.5–7.5), HEPES–NaOH (pH 7.5–8.5) and CHES–NaOH (pH 8.5–10.0). The ionic strength was maintained at constant value (0.033 M).

HPLC analysis: Mutants and WT proteins (in concentration from 0.1 to 0.5 μM) were incubated at 30 °C for times ranging from 1–24 h with 4-chlorocatechol and 4,5-dichlorocatechol (in concentration 10–200 μM) and the reaction mixtures were analysed by HPLC (Merck-Hitachi, with a Diode Array Detector) on a C_{18} reverse-phase column (model LiChrospher 100 RP-18), by using acetonitrile/water that contained H_3PO_4 (10 mM final pH 2.5; 50:50, *v/v*) as the solvent at a flow rate of 1 mL min^{-1}.[53] The reactions were stopped by the addition of concentrated H_3PO_4 to precipitate the protein and then centrifuged for 5 min at 10000 *g*. Mock reactions without the enzyme or without the substrates, which were incubated for the same times and in the same experimental conditions, were used as a control.

Demetallation: The metal ion removal was performed by employing a cationic exchanger resin IRC 50 Amberlite, which was functionalised with carboxylic groups (Sigma). The reaction conditions (resin treatment, protein concentration and incubation temperature) were as previously described.[33] Simultaneously a mock reaction was performed that contained only enzyme and buffer under the same conditions (without resin).

Statistical analysis: All data were obtained from the average of at least three independent experiments. The non-linear fittings were

calculated by using the version 9 software SigmaPlot (2004 Systat Software, Inc.).

Abbreviations: C1,2O: catechol 1,2-dioxygenase from *Acinetobacter radioresistens* S13; ADP1: *Acinetobacter calcoaceticus* ADP1; 3/4-CCD: 3/4-chlorocatechol 1,2-dioxygenase; *Rho* 1,2-CCD: 4-chlorocatechol 1,2-dioxygenase from *Rhodococcus opacus (erythropolis)* 1CP; *Ac* 1,2-CTD: catechol 1,2-dioxygenase from *Acinetobacter calcoaceticus* ADP1.

Acknowledgements

We are grateful to Cecilia Rosso for Figure 8.

Keywords: chloroaromatic degradation · cleavage reactions · metalloenzymes · oxidoreductases · protein engineering

[1] S. G. Burton, *Trends Biotechnol.* **2003**, *21*, 543–549.
[2] P. C. Cirino, F. H. Arnold, *Curr. Opin. Chem. Biol.* **2002**, *6*, 130–135.
[3] Z. Li, J. B. van Beilen, W. A. Duetz, A. Schmid, A. de Raadt, H. Griengl, B. Witholt, *Curr. Opin. Chem. Biol.* **2002**, *6*, 136–144.
[4] D. R. Boyd, N. D. Sharma, C. C. Allen, *Curr. Opin. Biotechnol.* **2001**, *12*, 564–573.
[5] N. Ogawa, K. Miyashita, A. M. Chakrabarty, *Chem. Rec.* **2003**, *3*, 158–171.
[6] P. W. Milligan, M. M. Haggblom, *Environ. Toxicol. Chem.* **1998**, *17*, 1456–1461.
[7] W. Reineke, *Annu. Rev. Microbiol.* **1998**, *52*, 287–331.
[8] D. H. Pieper, W. Reineke, *Curr. Opin. Biotechnol.* **2000**, *11*, 262–270.
[9] K. Furukawa, *J. Gen. Appl. Microbiol.* **2000**, *46*, 283–296.
[10] M. Dua, A. Singh, N. Sethunathan, A. K. Johri, *Appl. Microbiol. Biotechnol.* **2002**, *59*, 143–152.
[11] F. H. Vaillancourt, M. A. Haro, N. M. Drouin, Z. Karim, H. Maaroufi, L. D. Eltis, *J. Bacteriol.* **2003**, *185*, 1253–1260.
[12] G. R. Chaudhry, S. Chapalamadugu, *Microbiol. Rev.* **1991**, *55*, 59–79.
[13] J. Lin, M. Reddy, V. Moorthi, B. E. Qoma, *Afr. J. Biotechnol.* **2008**, *7*, 2232–2238.
[14] G. H. Lang, N. Ogawa, Y. Tanaka, T. Fujii, R. R. Fulthorpe, M. Fukuda, K. Miyashita, *Biochem. Biophys. Res. Commun.* **2005**, *332*, 941–948.
[15] C. H. Lin, H. T. Leow, S. C. Huang, J. Nakamura, J. A. Swemberg, P. H. Lin, *Chem. Res. Toxicol.* **2005**, *18*, 257–264.
[16] A. K. Pandey, M. Bajpayee, D. Parmar, R. Kumar, S. K. Rastogi, N. Mathur, P. Thorning, M. de Matas, Q. Shao, D. Anderson, A. Dhawan, *Environ. Mol. Mutagen* **2008**, *49*, 695–707
[17] N. Schweigert, S. Belkin, P. Leong-Morgenthaler, A. J. B. Zehnder, R. I. L. Eggen, *Environ. Mol. Mutagen.* **1999**, *33*, 202–210.
[18] N. Schweigert, A. J. Zehnder, R. I. Eggen, *Environ. Microbiol.* **2001**, *3*, 81–91.
[19] C. A. Earhart, M. W. Vetting, R. Gosu, I. Michaud-Soret, L. Que Jr. , D. H. Ohlendorf, *Biochem. Biophys. Res. Commun.* **2005**, *338*, 198–205.
[20] M. Ferraroni, I. P. Solyanikova, M. P. Kolomytseva, A. Scozzafava, L. Golovleva, F. Briganti, *J. Biol. Chem.* **2004**, *279*, 27646–27655.
[21] M. W. Vetting, D. H. Ohlendorf, *Structure* **2000**, *8*, 429–440.
[22] M. Ferraroni, M. P. Kolomytseva, I. P. Solyanikova, A. Scozzafava, L. A. Golovleva, F. Briganti, *J. Mol. Biol.* **2006**, *360*, 788–799.
[23] S. Liu, N. Ogawa, T. Senda, A. Hasebe, K. Miyashita, *J. Bacteriol.* **2005**, *187*, 5427–5436.
[24] P. Caposio, E. Pessione, G. Giuffrida, A. Conti, S. Landolfo, C. Giunta, G. Gribaudo, *Res. Microbiol.* **2002**, *153*, 69–74.
[25] S. Divari, F. Valetti, P. Caposio, E. Pessione, M. Cavaletto, E. Griva, G. Gribaudo, G. Gilardi, C. Giunta, *Eur. J. Biochem.* **2003**, *270*, 2244–2253.
[26] E. Griva, E. Pessione, S. Divari, F. Valetti, M. Cavaletto, G. L. Rossi, C. Giunta, *Eur. J. Biochem.* **2003**, *270*, 1434–1440.
[27] E. Pessione, S. Divari, E. Griva, M. Cavaletto, G. L. Rossi, G. Gilardi, C. Giunta, *Eur. J. Biochem.* **1999**, *265*, 549–555.
[28] F. Briganti, E. Pessione, C. Giunta, A. Scozzafava, *FEBS Lett.* **1997**, *416*, 61–64.
[29] F. Briganti, S. Mangani, L. Pedocchi, A. Scozzafava, L. A. Golovleva, A. P. Jadan, I. P. Solyanikova, *FEBS Lett.* **1998**, *433*, 58–62.
[30] E. Pessione, M. G. Giuffrida, R. Mazzoli, P. Caposio, S. Landolfo, A. Conti, C. Giunta, G. Gribaudo, *Biol. Chem.* **2001**, *382*, 1253–1261.
[31] F. Briganti, E. Pesione, C. Giunta, R. Mazzoli, A. Scozzafava, *J. Protein Chem.* **2000**, *19*, 709–716.
[32] T. Potrawfke, J. Armengaud, R. M. Wittich, *J. Bacteriol.* **2001**, *183*, 997–1011.
[33] G. Di Nardo, S. Tilli, E. Pessione, M. Cavaletto, C. Giunta, F. Briganti, *Arch. Biochem. Biophys.* **2004**, *431*, 79–87.
[34] M. Garcia-Viloca, J. Gao, M. Karplus, D. G. Truhlar, *Science* **2004**, *303*, 186–195.
[35] H. Zheng, J. D. Lipscomb, *Biochemistry* **2006**, *45*, 1685–1692.
[36] S. S. Katyare, S. P. Patel, H. R. Modi, *Neurochem. Res.* **2008**, *33*, 422–429.
[37] V. T. Maddaiah, C. L. Stemmer, S. Clejan, P. J. Collipp, *Biochim. Biophys. Acta, Enzymol.* **1981**, *657*, 106–121.
[38] T. Saku, S. Fushinobu, S. Y. Jun, N. Ikeda, H. Nojiri, H. Yamane, T. Omori, T. Wakagi, *J. Biosci. Bioeng.* **2002**, *93*, 568–574.
[39] S. Mehrotra, H. Balaram, *Biochim. Biophys. Acta, Proteins Proteomics* **2008**, *1784*, 2019–2028.
[40] A. P. Citadini, A. P. Pinto, A. P. Araújo, O. R. Nascimento, A. J. Costa-Filho, *Biophys. J.* **2005**, *88*, 3502–3508.
[41] T. D. H. Bugg, S. Ramaswamy, *Curr. Opin. Chem. Biol.* **2008**, *12*, 134–140.
[42] M. Xin, T. D. H. Bugg, *J. Am. Chem. Soc.* **2008**, *130*, 10422–10430.
[43] E. G. Kovaleva, J. D. Lipscomb, *Science* **2007**, *316*, 453–457.
[44] J. Schlosrich, K. L. Eley, P. J. Crowley, T. D. H. Bugg, *ChemBioChem* **2006**, *7*, 1899–1908.
[45] M. Velusamy, M. Palaniandavar, R. S. Gopalan, G. U. Kulkarni, *Inorg. Chem.* **2003**, *42*, 8283–8293.
[46] M. Velusamy, R. Mayilmurugan, M. Palaniandavar, *J. Inorg. Biochem.* **2005**, *99*, 1032–1042.
[47] P. C. A. Bruijnincx, M. Lutz, A. L. Spek, W. R. Hagen, B. M. Weckhuysen, G. van Koten, R. J. M. K. Gebbink, *J. Am. Chem. Soc.* **2007**, *129*, 2275–2286.
[48] Consolidated text of the articles of the law 11th October, 1986 No. 713 as updated by Legislative Decree 10th September 1991 No. 300 and by Legislative Decree 24th April, 1997 No. 126.
[49] R. W. W. Hooft, G. Vriend, C. Sander, E. E. Abola, *Nature* **1996**, *381*, 272.
[50] H. H. Hogrefe, J. Cline, G. L. Youngblood, R. M. Allen, *BioTechniques* **2002**, *33*, 1151–1165.
[51] L. Zheng, U. Baumann, J. L. Reymond, *Nucleic Acids Res.* **2004**, *32*, 114–115.
[52] G. Di Nardo, E. Pessione, M. Cavaletto, L. Anfossi, A. Vanni, F. Briganti, C. Giunta, *Biometals* **2004**, *17*, 699–706.
[53] M. Shimizu, K. Tetsuya, K. Takayoshi, K. Suzuki, N. Ogawa, K. Miyashita, K. Sakka, K. Ohmiya, *Appl. Environ. Microbiol.* **2002**, *68*, 4061–4066.

Received: December 19, 2008
Published online on March 19, 2009

